

Fatigue distribution optimization for offshore wind farms using intelligent agent control

Zhao, Rongyong; Shen, Wenzhong; Knudsen, Torben; Bak, Thomas

Published in:
Wind Energy

DOI (link to publication from Publisher):
[10.1002/we.1518](https://doi.org/10.1002/we.1518)

Publication date:
2012

Document Version
Early version, also known as pre-print

[Link to publication from Aalborg University](#)

Citation for published version (APA):

Zhao, R., Shen, W., Knudsen, T., & Bak, T. (2012). Fatigue distribution optimization for offshore wind farms using intelligent agent control. *Wind Energy*, 15(7), 927-944. <https://doi.org/10.1002/we.1518>

General rights

Copyright and moral rights for the publications made accessible in the public portal are retained by the authors and/or other copyright owners and it is a condition of accessing publications that users recognise and abide by the legal requirements associated with these rights.

- Users may download and print one copy of any publication from the public portal for the purpose of private study or research.
- You may not further distribute the material or use it for any profit-making activity or commercial gain
- You may freely distribute the URL identifying the publication in the public portal -

Take down policy

If you believe that this document breaches copyright please contact us at vbn@aub.aau.dk providing details, and we will remove access to the work immediately and investigate your claim.

RESEARCH ARTICLE

Fatigue distribution optimization for offshore wind farms using intelligent agent control

Rongyong Zhao¹, Wenzhong Shen², Torben Knudsen³ and Thomas Bak³

¹ CIMS Research Center, Tongji University, 200092 Shanghai, China

² Department of Wind Energy, Technical University of Denmark, 2800 Lyngby, Denmark

³ Department of Electronic Systems, Aalborg University, 9220 Aalborg, Denmark

ABSTRACT

A novel control approach is proposed to optimize the fatigue distribution of wind turbines in a large-scale offshore wind farm on the basis of an intelligent agent theory. In this approach, each wind turbine is considered to be an intelligent agent. The turbine at the farm boundary communicates with its neighbouring downwind turbines and organizes them adaptively into a wind delivery group along the wind direction. The agent attributes and the event structure are designed on the basis of the intelligent agent theory by using the unified modelling language. The control strategy of the intelligent agent is studied using topology models. The reference power of an individual wind turbine from the wind farm controller is re-dispatched to balance the turbine fatigue in the power dispatch intervals. In the fatigue optimization, the goal function is to minimize the standard deviation of the fatigue coefficient for every wind turbine. The optimization is constrained such that the average fatigue for every turbine is smaller than what would be achieved by conventional dispatch and such that the total power loss of the wind farm is restricted to a few percent of the total power. This intelligent agent control approach is verified through the simulation of wind data from the Horns Rev offshore wind farm. The results illustrate that intelligent agent control is a feasible way to optimize fatigue distribution in wind farms, which may reduce the maintenance frequency and extend the service life of large-scale wind farms. Copyright © 2012 John Wiley & Sons, Ltd.

KEYWORDS

wind turbine; fatigue; offshore wind farm; intelligent agent; optimization

Correspondence

Rongyong Zhao, CIMS Research Center, Tongji University, 200092 Shanghai, China.

E-mail: zhaorongyong@tongji.edu.cn

Received 4 April 2011; Revised 3 April 2012; Accepted 3 April 2012

1. INTRODUCTION

Because of the lack of suitable locations for wind turbines on land and the fact that the wind resource is more abundant at sea, offshore wind energy is increasingly being explored as a source of large-scale energy supply. Many projects are planned for wind farms with total outputs of more than 1000 MW. Thus, the offshore wind energy from an individual offshore wind farm project will reach an order of magnitude similar to a power station. Such developments have attracted the attention of the electricity supply industry.^{1–3}

The higher offshore energy yield is offset by higher construction, operation and maintenance costs; thus, the economic outcome is not necessarily better.^{4,5} Experience has demonstrated that the required maintenance time for offshore wind farms is significantly longer than for onshore installations. For example, according to Quinonez-Varela *et al.*,⁶ the estimated repair time of a failed subsea power cable may vary from 720 h in summer to 2160 h in winter. A large offshore wind farm, such as the one in Horns Rev, presents a new set of problems that have not been previously encountered, particularly, limited access to the farm because of weather conditions.⁷

One problem is the unbalanced fatigue distribution over the wind farm, which is caused by the uneven wind distribution and conventional wind farm control. This problem leads to frequent maintenance for the overloaded turbines located at boundaries of the wind farm, leading to high costs.

For a long period during the year, accessing the turbines by boat is difficult, and helicopters sometimes become the only suitable access mode. The cost of such visits is high and it is necessary to reduce the visit frequency. In this paper, we introduce an intelligent agent control concept to adaptively balance the loads on the wind turbines, synchronize the fatigue processes of the turbines and ultimately minimize the frequency of maintenance operations.

In Kristoffersen and Christiansen,¹ a wind farm main controller (WFMC) was developed on the basis of the desired type of control, the set points for the total active and reactive power, and dispatched power set points to the individual turbines. One of the control functions related to our topic is the balance control, which adjusts the farm power output to match the power requirements from the grid. However, the loads on the turbines are not balanced by the WFMC. In Fernandez *et al.*,⁸ wind farm control laws for the active and reactive power under normal conditions were studied. In Nilsson and Bertling,⁹ the condition monitoring systems were introduced to address the requirements for better maintenance management and to increase the reliability of the wind farm.

From the perspective of fatigue, wind turbines are the perfect 'fatigue machines'.¹⁰ To optimize wind turbine components with respect to fatigue life, Shirani and Håkegård engaged in the experimental determination and statistical analysis of the high-cycle fatigue properties of EN-GJS-400-18-LT ductile cast iron, which is mostly used in wind turbines.¹⁰ Marín *et al.*¹¹ studied the causes of failure (superficial cracks, geometric concentrators, abrupt changes of thickness) by using the simplified evaluation procedure for fatigue life from the 'Germanischer Lloyd' standard. From a probabilistic point of view, Sørensen *et al.*¹² evaluated the design code model in the wind turbine code [IEC 61400-1] and studied fatigue models relevant for welded, cast steel and fibre-reinforced details. Barle *et al.*¹³ studied the procedure for the service strength validation of stationary structures under wind loading, evaluated the static strength under a maximum monotonic load and assessed the fatigue under variable cyclic wind loads.

In order to reduce the fatigue loads of a single turbine, active control methods were proposed in van der Hooft *et al.*¹⁴ and Leithead *et al.*¹⁵ Leithead and Connor¹⁶ designed a control algorithm for variable speed wind turbines. Camblong¹⁷ developed an algorithm to minimize the wind disturbance impact on variable speed wind turbines. Lescher¹⁸ presented a multi-variable gain-scheduling controller designed from a linear parameter-varying representation of the non-linear wind turbine behaviour to alleviate wind turbine fatigue loads in the rated operating area. In Trudnowski and Lemieux,¹⁹ two separate real-time control algorithms were studied to reduce blade fatigue cycle amplitudes caused by wind shear and gravity effects. In Kallesøe,²⁰ a new low-order mathematical model was introduced to analyse blade dynamics and blade load-reducing control strategies for wind turbines. Heege *et al.*²¹ calculated the dynamic loads of wind turbine power trains, with particular emphasis on planetary gearbox loads. Veldkamp *et al.*²² examined the differences in fatigue for certain representative offshore wind turbines. In Thomsen and Soerensen,²³ the increased fatigue loading in a wind farm, in comparison with the one in free air, was found to be between 5% and 15%, depending on the wind farm layout.

To date, most of the developments within control algorithms and technologies have focused on wind farm power control and the fatigue reduction of a single turbine. However, operation of offshore wind farms show that the individual active control method cannot solve the unequal fatigue distribution in the wind farm. If a control algorithm or technology can take into account the fatigue distribution and balance the individual turbine fatigue without a large power loss, then it can be used to reduce the maintenance costs and increase the wind farm service life.

To solve this problem, we describe an offshore wind farm model and define a fatigue coefficient to measure the fatigue accumulation. The present work uses the concept of intelligent agent control^{24,25} and game theory²⁶ to dynamically model a multi-intelligent agent network.

In artificial intelligence control, an intelligent agent is an autonomous entity that observes through sensors and acts upon an environment by using actuators. It directs its activity towards achieving goals, and it may learn to achieve the goals.²⁴ Intelligent agent controls have their own simple communication, negotiation and logic control. In this work, each wind turbine is considered to be an intelligent agent. The turbine at the farm boundary communicates with its neighbouring downwind turbines and organizes them adaptively into a wind delivery group along the wind direction. The advantages of an intelligent agent control are the properties of autonomy, scalability, reactivity and proactivity.²⁴

The power reference of each wind turbine is re-dispatched according to its fatigue coefficient. This fatigue optimization is a constrained problem. The goal is to minimize the standard deviation of the fatigue factor of each wind turbine. Two constraints are considered: the average fatigue for every turbine should be smaller than one with conventional control and the power loss of the wind farm should be restricted to a few per cent of the total power.

In Section 2, a typical wind farm model and definitions for fatigue assessment are presented. The system description in Section 2 is not intended to contribute to the state of art in wind farm modelling but is intended to define the minimal necessary components and complexity required to test the performance of the proposed wind farm control method. The intelligent agent control model is studied in Section 3 for fatigue optimization in a wind farm. In Section 4, the workflow of intelligent agent control is presented. Numerical simulation of the present mathematical model is shown in Section 5. Section 6 discusses the possible ratios of the disturbance fatigue to the working fatigue, corresponding to possible wind conditions and wind farm layouts. Finally, the conclusions are drawn in Section 7.

2. SYSTEM DESCRIPTIONS

In large-scale offshore wind farms, the mean wind speed decreases at the turbines clustered in the downwind direction. According to Frandsen,²⁷ initial efforts have been made to estimate the wind speed reduction in a large cluster of wind turbines.^{28–32} In general, the distance between two neighbouring turbines in large-scale offshore wind farms is approximately 5–8 rotor diameters, representing a large distance in practice.^{33–35} We consider a typical offshore wind farm with a matrix layout of m rows and n columns, as illustrated in Figure 1. The farm layout model uses a regular array geometry with straight rows of wind turbines and equidistant spacing between the turbines in each row and each column. Figure 1 shows an example of the array geometry taken from the Horns Rev offshore wind farm. Each turbine marked with $A(i, j)$ acts as an intelligent agent used to communicate and negotiate with other turbines through an intranet. The indices of i ($i = 1, 2, \dots, m$) and j ($j = 1, 2, \dots, n$) are the row and column variables, respectively.

Under the far wake condition, we consider first the basic case in which the wind direction is parallel to the columns in a rectangular geometry, as in Frandsen.²⁷ In other words, the wake influence exists only in a turbine line downwind.

We take an arbitrary agent $A(i, j)$ as an example shown in Figure 1. $A(i, j)$ receives the wind energy that remains from the upstream turbine agents of $A(i-1, j)$, $A(i-2, j)$, \dots and $A(1, j)$. Then, after the negotiation, the wind turbine agent $A(i, j)$ can also leave some wind energy for the downstream wind turbine agents $A(i+1, j)$, $A(i+2, j)$, \dots and $A(m, j)$.

In order to model the wind energy redistribution relationship, several basic definitions are described, as follows, on the basis of the Betz's elementary momentum theory.³

2.1. Front wind power

The wind energy in front of agent $A(i, j)$, i.e. the upwind power in front of the turbine (i, j) , is

$$P_{fro}(i, j) = \frac{1}{2} \rho v_{i,j}^3 S \quad (1)$$

where ρ is the air density, $v_{i,j}$ is the wind speed in front of the turbine (i, j) and S is the area swept by the turbine blades. The wind power in front of agent $A(i+1, j)$ is

$$P_{fro}(i+1, j) = \frac{1}{2} \rho v_{i+1,j}^3 S \quad (2)$$

In order to estimate the wind speed deficit at any downwind distance, a model of the wake expansion needs to be established. There exists a relationship between the wind speed and the downwind distance. The ratio between the wind speed in front of $A(i, j)$ and the wind speed in front of $A(i+1, j)$ is naturally dependent on different factors, e.g. the thrust

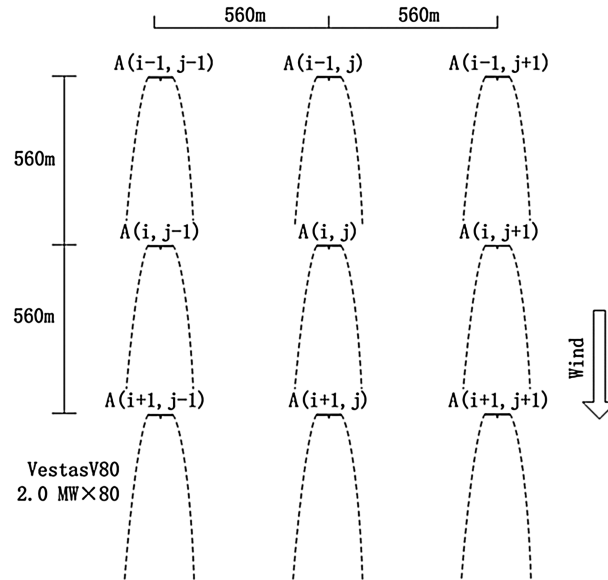


Figure 1. Wind farm model under the far wake condition at the Horns Rev offshore wind farm.

coefficient of the wind turbines, atmospheric turbulence, wake turbulence mixing and the wake expansion coefficient. On the basis of the model constants used in the Frandsen model, the Schlichting model, the Jensen model and the Schlichting model without linearization of the momentum equation,²⁷ we employ the averaged value of the four constants for the ratio between the wind speed in front of $A(i, j)$ and the wind speed in front of $A(i + 1, j)$ at a distance of seven rotor diameters as follows, assuming a wind speed in the range of $2\text{--}24\text{ m s}^{-1}$,

$$\frac{v_{i+1,j}}{v_{i,j}} = 0.9288 \quad (3)$$

This value is approximately equal to that obtained in Vermeera *et al.*,³³ which was determined using actual engineering experiences with velocity deficits in the far wake. It should be noted that other ratios different from the value given in Equation (3) can also be used in our model, and the precise value should be determined from the actual wind conditions and farm layout.

2.2. Wind delivery coefficient

In this section, the wind delivery coefficient is defined as the ratio of the wind power in front of a downwind turbine to the one in front of its upwind partner. According to the wind direction, this coefficient can be divided into two categories: a normal delivery coefficient and an oblique delivery coefficient.

2.2.1. Category 1. Normal delivery coefficient.

To study the delivery coefficient, we consider the first category of cases in which the wind is normal to the wind farm layout. We assume that any downwind turbine can only absorb part of the wind energy along the wind direction that is left after absorption by the upwind turbines in the same column. These cases are shown in Figure 2, with the main wind directions of 0° , 90° , 180° and 270° . The normal wind delivery coefficient is defined as the ratio α_0 of the wind power in front of $A(i + 1, j)$ to the wind power in front of $A(i, j)$ at a distance of seven rotor diameters

$$\alpha_0 = \frac{P_{fro}(i + 1, j)}{P_{fro}(i, j)} = \frac{\frac{1}{2}\rho v_{i+1,j}^3 S}{\frac{1}{2}\rho v_{i,j}^3 S} = \frac{v_{i+1,j}^3}{v_{i,j}^3} = 0.8012 \quad (4)$$

Using Equation (4), we can deduce the wind power relationship between turbines in the same column

$$P_{fro}(i + k, j) = \alpha_0^k P_{fro}(i, j) = 0.8012^k P_{fro}(i, j) \quad (5)$$

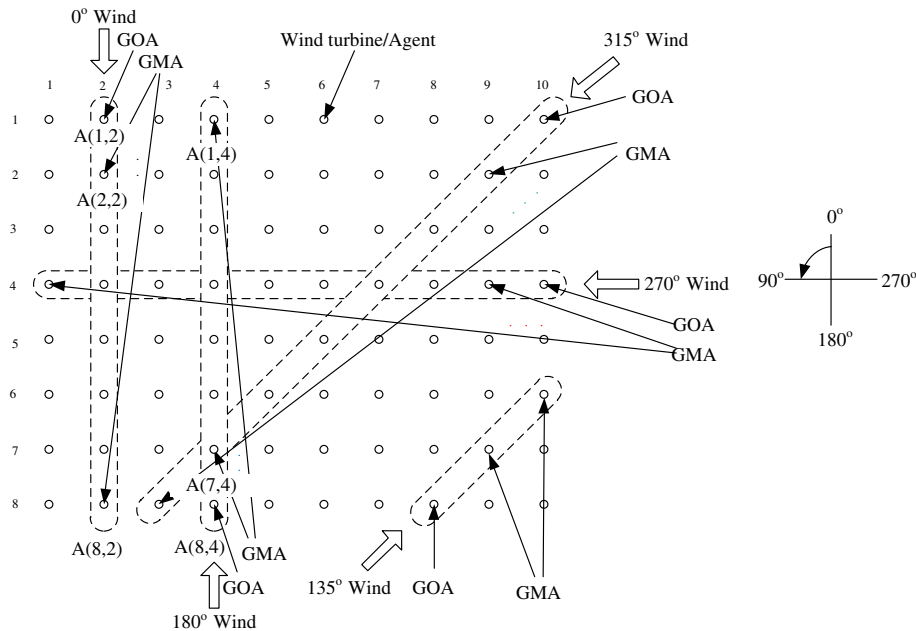


Figure 2. Agent group organization for wind turbines at the Horns Rev offshore wind farm.

where $k = 1, 2, \dots, m - i$. Equation (5) shows a relationship between the wind power $P_{fro}(i + k, j)$ and $P_{fro}(i, j)$ in the function of the constants k and α_0 . When an upwind turbine leaves some wind energy, $\Delta P_{fro}(i, j)$, for the downwind turbine, the power delivery will be

$$\Delta P_{fro}(i + k, j) = \alpha_0^k \Delta P_{fro}(i, j) = 0.8012^k \Delta P_{fro}(i, j) \quad (6)$$

We can now discuss the relationship between the electric power from the wind turbine agents (i, j) and $(i + k, j)$. In Hau,⁴ the reference power, $P_{ref}(i, j)$, is the electric power dispatched by the WPMC, and the wind turbine can generate the power according to the power-wind speed curve

$$P_{ref}(i, j) = c_p P_{fro}(i, j) \quad (7)$$

where c_p is the power coefficient. Under partial-load conditions that are the most common for wind turbine operation, c_p is almost constant. Under full-load conditions, c_p can be assumed to follow a piecewise linear function.⁴ Thus, we can calculate the change in electric power as

$$\Delta P(i, j) = \Delta P_{ref} = c_p \Delta P_{fro}(i, j) \quad (8)$$

Further, on the basis of Equations (6) and (8), we have

$$\Delta P(i + k, j) = \alpha_0^k \Delta P(i, j) = 0.8012^k \Delta P(i, j) \quad (9)$$

Equation (9) gives

$$\Delta P(i, j) > 0 \Rightarrow \Delta P(i + k, j) > 0 \quad (10)$$

If a change in power $\Delta P(i, j)$ is needed for turbine (i, j) , artificial wind energy delivery occurs, i.e. the upwind turbine agent $A(i, j)$ gives up a part of its wind power to its downwind partner, the turbine agent $A(i + k, j)$, and then,

$$\Delta P(i, j) < 0 \Rightarrow \Delta P(i + k, j) > 0 \quad (11)$$

It should be noted that when an upwind turbine is more fatigued than the downwind turbine, it can always give some wind energy to its downwind turbine by adjusting its pitch angle or rotational speed, depending on whether or not the wind speed has reached its rated value. In addition, we assume that $\Delta P(i, j)$ is positive for simplicity in the next sections.

2.2.2. Category 2. Oblique delivery coefficient.

In order to simplify the situation caused by the changes in wind direction, other main wind directions of 45° , 135° , 225° and 315° , which are oblique to the wind farm layout, are considered. These cases are shown in Figure 2. The distance between the neighbouring upwind and downwind turbines is $x = 7\sqrt{2}D$ (D is the rotor diameter). With the same calculation method as Equation (3), which was verified in Vermeera *et al.*,³³ the corresponding ratio of the upwind and downwind speeds is 0.9415. The ratio α_1 , i.e. the oblique wind delivery coefficient, of the wind power in front of $A(i, j)$ to the one in front of $A(i + 1, j)$ at a distance of $7\sqrt{2}D$ is

$$\alpha_1 = \frac{P_{fro}(i + 1, j + 1)}{P_{fro}(i, j)} = \frac{\frac{1}{2}\rho v_{i+1,j+1}^3 S}{\frac{1}{2}\rho v_{i,j}^3 S} = \frac{v_{i+1,j+1}^3}{v_{i,j}^3} = 0.8346 \quad (12)$$

Using Equation (12), we can deduce the wind power relation between turbines in any oblique turbine column

$$P_{fro}(i + k, j + k) = \alpha_1^k P_{fro}(i, j) = 0.8346^k P_{fro}(i, j) \quad (13)$$

where $k = 1, 2, \dots, m - i$. When an upwind turbine gives up some wind power, $\Delta P_{fro}(i, j)$, to an oblique downwind turbine, the power delivery will be

$$\Delta P_{fro}(i + k, j + k) = \alpha_1^k \Delta P_{fro}(i, j) = 0.8346^k \Delta P_{fro}(i, j) \quad (14)$$

The relationship between the electric power of wind turbine agents (i, j) and $(i + k, j + k)$ can be calculated using Equation (9):

$$\Delta P(i + k, j + k) = \alpha_1^k \Delta P(i, j) = 0.8346^k \Delta P(i, j) \quad (15)$$

It is worth noting that the power delivery coefficients in both the normal and oblique wind directions are theoretical parameters.

2.3. Fatigue coefficient

In order to balance and optimize the fatigue of the turbines in an offshore wind farm, an integrated and quantitative parameter should be defined to measure the fatigue of an individual turbine. In general, the more power a turbine generates the higher fatigue. The turbine fatigue should also include a component that reflects the incoming turbulence. For example, in the wake of another turbine, a turbine may produce low electric power but experiences more turbulence, which results in higher fatigue loads.

On the basis of the experimental data and the statistical analysis of the fatigue properties of EN-GJS-400-18-LT ductile cast iron from Shirani and Häkegård,¹⁰ the simplified evaluation procedure of the fatigue life by Marín *et al.*,¹¹ and the fatigue under variable cyclic wind loads by Barle *et al.*,¹³ we assume that the fatigue is mainly caused by the wind disturbance mixed into the real wind flow with random frequencies. Therefore, a reasonable definition of fatigue should take both working power fatigue and wind disturbance fatigue into account.

This study takes the rated power, the generated power, the wind turbulence and the service life of a wind turbine into account. Here, we calculate the total power that a turbine has generated from the day of installation ($t = 0$) to the present ($t = t_p$). We refer to the calculation of the effective turbulence intensity proposed in Thomsen and Soerensen²³ and then define the fatigue coefficient of a turbine as

$$C_{fat} = f_{work} + f_{dis} = \frac{\int_0^{t_p} p(t)dt}{P_{rat}T_{ser}(1 + p_{refp})} + C_{dis} \frac{\int_0^{t_p} I_{eff}(t)dt}{T_{ser}(1 + p_{refp})} \quad (16)$$

In Equation (16), C_{fat} is the fatigue coefficient of a turbine and consists of two parts: i) f_{work} , the fatigue caused by the power generation, referred to as the working fatigue, and ii) f_{dis} , the fatigue caused by the wind turbulence disturbance, referred to as the disturbance fatigue. Here, $p(t)$ is the power at the instant of time t . P_{rat} is the rated power of a specific turbine; T_{ser} is the designed service life of a turbine, e.g. 20 years or 25 years; and p_{refp} is the reparation coefficient for normal maintenance, which takes a value between 0 and 1. It is obvious that the service duration will possibly be extended when components are repaired or replaced. Therefore, p_{refp} is an empirical parameter that depends on the importance of key components in ensuring power generation fatigue, and C_{dis} is the disturbance coefficient, which is a constant, determined by the wind farm layout, the wind turbine material structure and the local climate factors. In calculations at a local wind farm site, the curve for the measured multi-wake in Figure 4 of Thomsen and Soerensen²³ should be adapted according to the measured wind speed data. $I_{eff}(t)$ is the effective turbulence intensity. Thomsen and Soerensen²³ describe a method that is often used to include wake effects in the turbulence intensity. It involves determining the effective turbulence intensity, $I_{eff}(t)$, from the ambient turbulence intensity, $I_a(t)$, and the wake turbulence intensity contribution, $I_w(t)$, as follows

$$I_{eff}(t) = \sqrt{I_a(t)^2 + I_w(t)^2} \quad (17)$$

According to Thomsen and Soerensen,²³ the wake turbulence intensity contribution, $I_w(t)$, is calculated as

$$I_w(t) = \frac{1}{S} \sqrt{1.2C_t(t)} \quad (18)$$

where S is the turbine spacing in the number of rotor diameters and $C_t(t)$ is the wind turbine thrust coefficient. The turbulence intensity curves of the free flow and multi-wake regions in Figure 4 of Thomsen and Soerensen²³ also show that the average turbulence ratio of the free flow to multi-wake regions is nearly 1:1.7032.

In material science, fatigue is the progressive and localized structural damage that occurs when a material is subjected to cyclic loading.²³ The fatigue of a wind turbine is a very complex quantity. However, the natural frequent loading and unloading of a complete wind turbine structure by the wind and wake disturbances are the main causes of potential fatigue. Therefore, to simplify the complex fatigue calculation, we mainly consider the disturbance fatigue and the working fatigue. When electric power is generated, the relationship between the working fatigue and the disturbance fatigue is defined by

$$\gamma = f_{dis}/f_{work} \quad (19)$$

where γ is the ratio of the disturbance fatigue(f_{dis}) to the working fatigue(f_{work}), which are determined from the wind farm layout and the local wind conditions. As shown in Equation (17), the disturbance fatigue is generated by two sources: the original atmospheric wind disturbance, noted as $I_a(t)$, and the original wind disturbance superimposed by the wake turbulence when a turbine operates in an area of the wake from the upwind turbine(s), noted as $I_w(t)$. Therefore, the disturbance fatigue, f_{dis} , is determined by both the wind farm layout and the climate conditions. On the other hand, the working fatigue, f_{work} , is caused by the power generation and is affected by the rated power, the turbine service life and the reparation coefficient; therefore, it is mainly determined by the wind conditions. Further, the wake-added turbulence

is not small. The increased fatigue loading in the wind farm, compared to the free flow, was found to be between 5% and 15%, depending on the wind farm layout.²³

Now, Equation (16) can be changed into the calculation of the fatigue coefficient

$$C_{fat} = \begin{cases} C_{fat}(t_0) + f_{work} + f_{dis} = C_{fat}(t_0) + (1 + \gamma) \frac{\int_{t_0}^{t_p} p(t) dt}{P_{rat} T_{ser}(1 + p_{refp})}, & \text{if } v_{cut-in} < v < v_{cut-off} \\ C_{fat}(t_0) + f_{dis} = C_{fat}(t_0) + C_{dis} \frac{\int_{t_0}^{t_p} I_{eff}(t) dt}{T_{ser}(1 + p_{refp})}, & \text{if } v < v_{cut-in} \text{ or } v > v_{cut-off} \end{cases} \quad (20)$$

Here, $C_{fat}(t_0)$ is the fatigue coefficient of a turbine at time t_0 . A wind turbine does not operate when the wind velocity is outside of the wind speed range (v_{cut-in} , $v_{cut-off}$).

3. DESIGN OF THE INTELLIGENT AGENT MODEL

3.1. Game logic variables

On the basis of the game theory,^{24,25} we define two Boolean variables that determine whether an upwind turbine can deliver wind power to the downwind turbine and whether a downwind turbine can accept the request from the upwind turbine.

Case 1: normal delivery. In the case of a normal delivery, the equation used in determining whether an agent $A(i, j)$ will deliver its wind power to its downwind agent $A(i + k, j)$ is

$$\xi(i, j, k) = \begin{cases} 1, & \text{if } A(i, j) \text{ will deliver wind power to } A(i + k, j) \\ 0, & \text{if } A(i, j) \text{ will not deliver wind power to } A(i + k, j) \end{cases} \quad (21)$$

where k ($k = 1, 2, \dots, m - i$) is the skipping number between the upwind turbine and its partner. A second equation is defined to determine whether or not an agent $A(i + k, j)$ will accept the wind power from its upwind agent $A(i, j)$:

$$\sigma(i, j, k) = \begin{cases} 1, & \text{if } A(i + k, j) \text{ will accept wind power from } A(i, j) \\ 0, & \text{if } A(i + k, j) \text{ will not accept wind power from } A(i, j) \end{cases} \quad (22)$$

When the basic negotiation variables are designed, the amount of wind power that should be delivered can be determined according to the fatigue coefficient, C_{fat} , the current wind speed and the reference power dispatched by the WPMC.

Case 2: oblique delivery. In the case of an oblique delivery, the equation that is defined on the basis of whether an agent $A(i, j)$ will deliver its wind power to its downwind agent $A(i + k, j + k)$ is

$$\xi(i, j, k) = \begin{cases} 1, & \text{if } A(i, j) \text{ will deliver wind power to } A(i + k, j + k) \\ 0, & \text{if } A(i, j) \text{ will not deliver wind power to } A(i + k, j + k) \end{cases} \quad (23)$$

A second equation is defined to determine whether an agent $A(i + k, j + k)$ will accept the wind power from $A(i, j)$

$$\sigma(i, j, k) = \begin{cases} 1, & \text{if } A(i + k, j + k) \text{ will accept wind power from } A(i, j) \\ 0, & \text{if } A(i + k, j + k) \text{ will not accept wind power from } A(i, j) \end{cases} \quad (24)$$

3.2. Intelligent agent model

In order to organize the wind turbines into different wind delivery groups, two types of agents are defined (see Figure 2): a group organizer agent (GOA) and a group member agent (GMA). The GOA judges the present wind direction, sends the group organization request signal to all of the downwind turbines along the wind direction and then organizes them into a wind delivery group including the GOA itself. At any time, the wind delivery groups are independent of each other, such that any wind delivery between the GOA and the GMA only occurs within the same group. According to Russell and Norvig, Krishna and Ramesh, and Bryant and Miikkulainen,^{24–26} any wind turbine can theoretically act as a GOA or a GMA. We define the boundary turbines as GOA agents and all inside turbines as GMA agents on the basis that wind can only blow from a farm boundary to the inside of a farm.

The agent group organization method is shown in Figure 2. If 45° is assumed to be the angle interval, there are eight main directions that can be divided into two categories. Groups are organized by the GOAs on the boundary that faces the wind according to the present wind direction. As an example, see the group in Figure 2 bounded by a dash line for the case when the wind direction is 0° , i.e. the wind is blowing from top to bottom. $A(1,2)$ acts as the group organizer agent, i.e. the

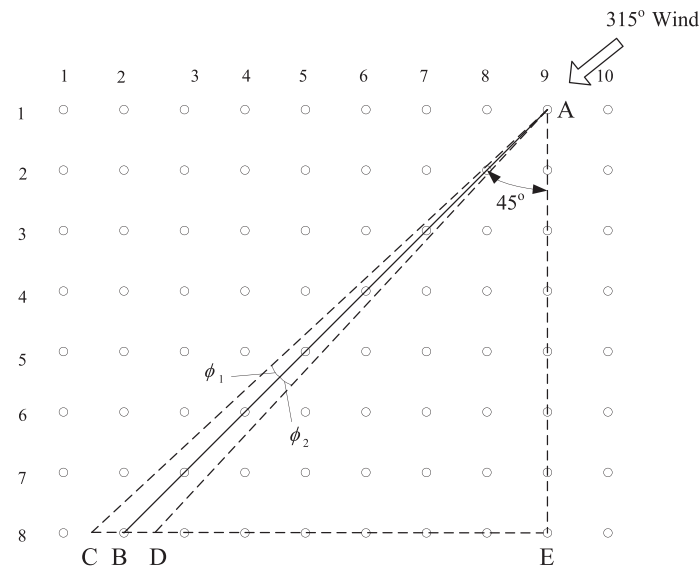


Figure 3. Angle tolerance for a wind direction of 315° at the Horns Rev offshore wind farm.

GOA. All other turbines $A(kk, 2)$ ($kk = 2, 3, \dots, 8$) act as GMAs. The same group organization occurs simultaneously in other columns. When the wind direction changes to 180° , as for the second group shown in Figure 2, the bottom turbine $A(8,4)$ will act as the GOA. All other turbines $A(kk, 4)$ ($kk = 7, 6, \dots, 1$) will act as GMAs and vice versa.

In order to simplify the possible wind directions according to the dynamic group organization, the angle tolerance is considered. We define the angle tolerance as the changes in wind direction around the main wind directions (0° , 90° , 180° , 270° , 45° , 135° , 225° and 315°), in which all of the downwind turbines can be included in the wake area of the upwind turbines for a single wind direction, as shown in Equation (28). In Figure 3, it is reasonable to keep the wake boundary points in the middle of the last two downwind turbine agents.

The minimum permissive tolerance (see Figure 3) for wind at 315° can be determined by comparing the permissive wind direction fluctuations in different areas. The permissive left angle, ϕ_1 , is

$$\phi_1 = \tan^{-1} \left(\frac{CE}{EA} \right) - 45^\circ = \tan^{-1} \left(\frac{0.5 \times 7D + 7 \times 7D}{7 \times 7D} \right) - 45 = 1.9749^\circ \quad (25)$$

The permissive right angle, ϕ_2 , is

$$\phi_2 = 45^\circ - \tan^{-1} \left(\frac{DE}{EA} \right) = 45^\circ - \tan^{-1} \left(\frac{0.5 \times 7D + 6 \times 7D}{7 \times 7D} \right) = 2.1211^\circ \quad (26)$$

Now, the wind angle tolerance is obtained as

$$A_{tol} = \pm \min\{\phi_1, \phi_2\} = \pm 1.9749^\circ \quad (27)$$

On the basis of the calculation mentioned, the tolerances in the other main wind directions of 0° , 45° , 90° , 180° , 225° and 270° are calculated to be

$$A_{tol} = \begin{cases} \pm 4.0856^\circ, \theta_{wind} = 0^\circ, 180^\circ \\ \pm 1.9749^\circ, \theta_{wind} = 45^\circ, 135^\circ, 225^\circ, 315^\circ \\ \pm 2.8624^\circ, \theta_{wind} = 90^\circ, 270^\circ \end{cases} \quad (28)$$

3.3. Intelligent agent structure definition

The class structures of the GOAs and the GMAs are designed according to the actual turbine attributes and the intelligent agent structure requirements in the unified modelling language.³⁶ Both types of agents have three attribute categories: private attributes, public attributes and events (see Figure 4). Private attributes refer to all the attributes that are only owned and accessed by the subject itself. For example, as a GOA subject, a wind turbine has private attributes: the rated power, the

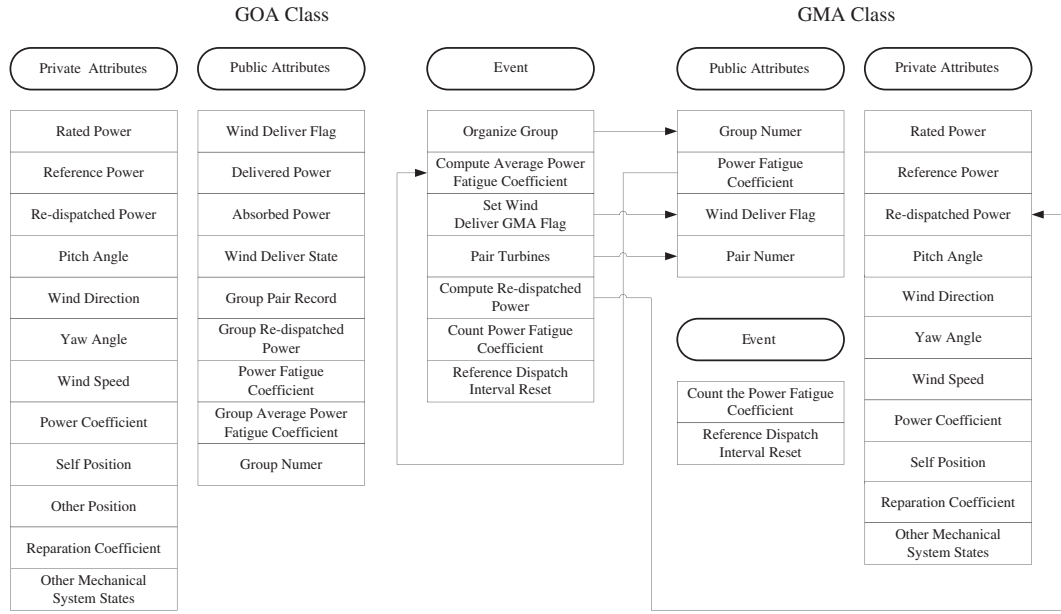


Figure 4. Intelligent agent class definition.

reference power dispatched by the farm controller, the pitch angle etc. Public attributes correspond to all of the attributes accessed by both the owner agent and the other agents, and include the wind delivery flag, the delivered power, etc. Events correspond to all of the events or functions executable by the owner agent, such as organize group, computing the average fatigue coefficient, etc.

In Figure 4, the two classes (GOA and GMA) of intelligent agents are shown. The GOA structure is more complicated than the GMA structure, and the GOA has more private attributes, public attributes and events than the GMA. For example, the other position in the GOA private attributes refers to the geographic information for all other turbines saved in the GOA controller memory, the group pair record in the GOA public attributes records all of the wind delivery and wind absorbing turbines in a single group in pairs by their numbers, and the organizer group of the GOA events is exclusively owned by the GOA.

There exists an obvious relationship in the input and the output of the GOA and the GMA. The output of the GOA event organizer group is a group number, which is one of the public attributes of the GMA. The fatigue coefficient attribute of the GMA is the input to the compute average fatigue coefficient event of the GOA. The output of the set wind deliver GMA flag event determines the wind deliver flag of the GMA. The pair turbines event outputs the pair number of the GMA. The compute re-dispatched power event outputs the re-dispatched power of the GMA.

3.4. State topology

In order to balance the fatigue, it is necessary for both the GOA and GMA to obtain their re-dispatched power. Therefore, a power control topology should be designed, as shown in Figures 5 and 6. The GOA owns four states in total. In Mode 1, the expression $P_{out} = P_{ref}$ means that the output power equals the reference power dispatched from the WPMC, which is the initial power of each turbine, determined using the same method as in the conventional control approach without fatigue balance. In Mode 2, $GroupNumber = kk$ indicates that the GOA organizes the wind turbine group in a power-dispatching interval, e.g. 20 min. In this state, every group member agent (turbine) will be marked with kk ($kk = 1, 2, \dots, kkmax$) in their $GroupNumber$ variable. Here, $kkmax$ is the maximum group number, which changes adaptively with the wind direction. When the wind direction angles are 0° or 180° , $maxkk$ is equal to 8. When the wind direction angles are 45° , 135° , 225° or 315° , $kkmax$ is equal to 17. In this case, the minimum group consists of only one GOA, which is located at the two ends of the wind farm where wind delivery does not occur. The top turbines just keep their initial reference power. When the wind direction angles are 90° or 270° , $maxkk$ is equal to 10.

In Mode 3, $P_{out}(ll, kk) = Pre-dispatched(ll, kk)$ indicates that all of the turbine agent group members, including the GOA itself, are re-dispatched by the GOA. In Mode 4, $P_{out} = P_{ref} - \Delta P$ indicates a possible re-dispatch result. The

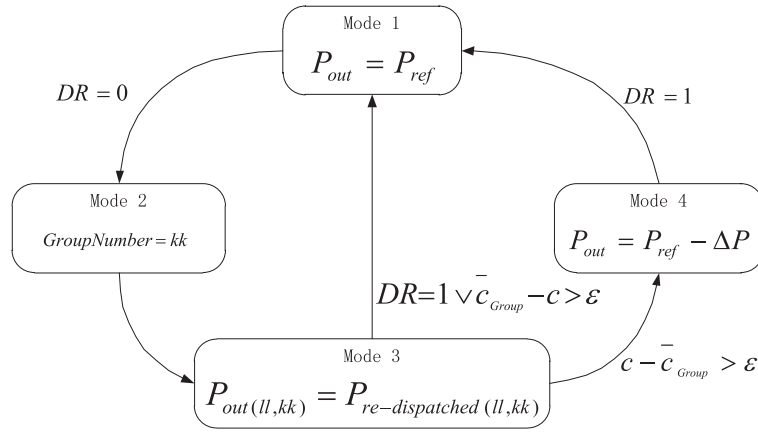


Figure 5. GOA power control topology.

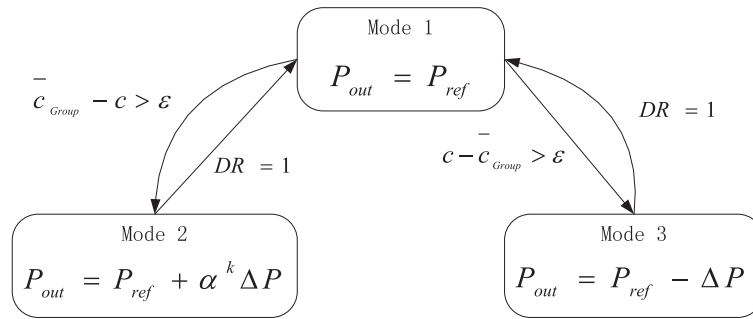


Figure 6. GMA power control topology.

GOA leaves some wind energy to one of the downwind member agents. Here, P_{ref} is the initial reference power, and ΔP is the power decrease ordered by the GOA. In order to keep P_{out} positive, ΔP is calculated as

$$\Delta P = \begin{cases} 2(P_{ref} - \overline{P_{kk}}), & \text{if } P_{ref} - 2(P_{ref} - \overline{P_{kk}}) > 0 \\ 0.5P_{ref}, & \text{otherwise} \end{cases} \quad (29)$$

where $\overline{P_{kk}}$ is the average power of the wind delivery group kk . In most cases, ΔP is equal to the upper value. In the few cases in which the reference power, P_{ref} , is too large to keep P_{out} positive, we directly set ΔP equal to the half of P_{ref} . All the state transfer guards at the edges are shown in Figures 5 and 6. DR is the dispatch reset signal triggered by the WPMC. $DR = 0$ indicates that the reference power dispatch process is complete and that all turbine agents have received their task to generate the reference value electric power. The GOAs will trigger the group organizing event simultaneously in Mode 2.

The guard $DR = 1$ indicates that all turbine agents will be reset to the initial state, Mode 1. In the GOA topology, there is a non-conditional state transfer from Mode 2 to Mode 3, which means that Mode 3 will take place immediately if Mode 2 does not have the sufficient conditions to judge.

The guard $DR = 1 \vee \overline{c_{Group}} - c > \varepsilon$ indicates that either $DR = 1$ or $\overline{c_{Group}} - c > \varepsilon$ occurs. $\overline{c_{Group}} - c > \varepsilon$ indicates that the present turbine agent suffers less fatigue in the agent group. c is equal to the fatigue coefficient c_{fat} . The guard $c - \overline{c_{Group}} > \varepsilon$ means that the present turbine agent suffers more fatigue in the agent group. In the GMA topology shown in Figure 6, the obvious differences from the GOA are in Mode 2, the power adding mode and some state transfer conditions. In Mode 2, $P_{out} = P_{ref} + \alpha^k \Delta P$ indicates that the present GMA absorbs some power. $\alpha^k \Delta P$ is the added power, ΔP is the power decrease associated with one of the upwind turbine agents in the same group, and α is the wind delivery coefficient, which could be $\alpha_0 = 0.8012$ or $\alpha_1 = 0.8346$, depending on the wind direction described previously.

The superscript k of α denotes the number of turbines skipped between the pair of turbine agents.

Note that all the power re-dispatch states only occur within a reference power dispatch interval from the WPMC, in which the signal DR remains zero. In other words, the signal DR is set to 1 when a new farm power dispatch interval

begins. When the signal DR is equal to 1, the turbine agent should immediately be reset to its initial state, Mode 1, no matter which wind delivery states the GOA or GMA is operating in.

3.5. Fatigue optimization

The goal of intelligent agent-based optimization is to balance the fatigue distribution evenly in a wind farm. Mathematically, the optimization problem subject to constraints is

$$\begin{aligned} \min\{st(C_{fat})\} &= \min \left\{ \sqrt{\frac{1}{mn} \left(\sum_{i=1}^m \sum_{j=1}^n (C_{fat}(i, j) - \overline{C_{fat}})^2 \right)} \right\} \\ \text{subject to } st_i(C_{fat}) &\leq \varepsilon_{st}, i = 1, \dots, n_{total} \\ (\overline{C_{fat}})_{balance_i} &< (\overline{C_{fat}})_{conventional_i}, i = 1, \dots, n_{total} \\ P_{loss_i} &< \eta P_{farm_i}, i = 1, \dots, n_{total} \end{aligned} \quad (30)$$

where $st(C_{fat})$ is the standard deviation considered as the objective function to be minimized over the variable i . $\overline{C_{fat}}$ is the average fatigue of all turbines, i.e. the mean fatigue in Figures 8, 9 and 10 in Section 5. The first inequality $st(C_{fat}) \leq \varepsilon_{st}$ is an optimization goal, where n_{total} is the calculation time; ε_{st} is the tolerance, which is chosen to be 0.001 in this work. The second inequality $(\overline{C_{fat}})_{balance_i} < (\overline{C_{fat}})_{conventional_i}$ is the second constraint, which means that the average balanced fatigue should be smaller than the average fatigue by conventional control. The third inequality is $P_{loss_i} < \eta P_{farm_i}, i = 1, \dots, n_{total}$, which means that the power loss of the wind farm is restricted, which should be smaller than η times of the dispatched power P_{farm_i} of the wind farm in every interval. Empirically, we set $\eta = 5\text{--}10\%$.

4. WORKFLOW OF INTELLIGENT AGENT CONTROL

On the basis of the mentioned control topology, the workflow of the GOA is outlined in Figure 7. In the state initialization process, each turbine agent measures its local wind direction $\mu_{wind}(i; j)$ and the wind speed $v_{wind}(i; j)$, and obtains

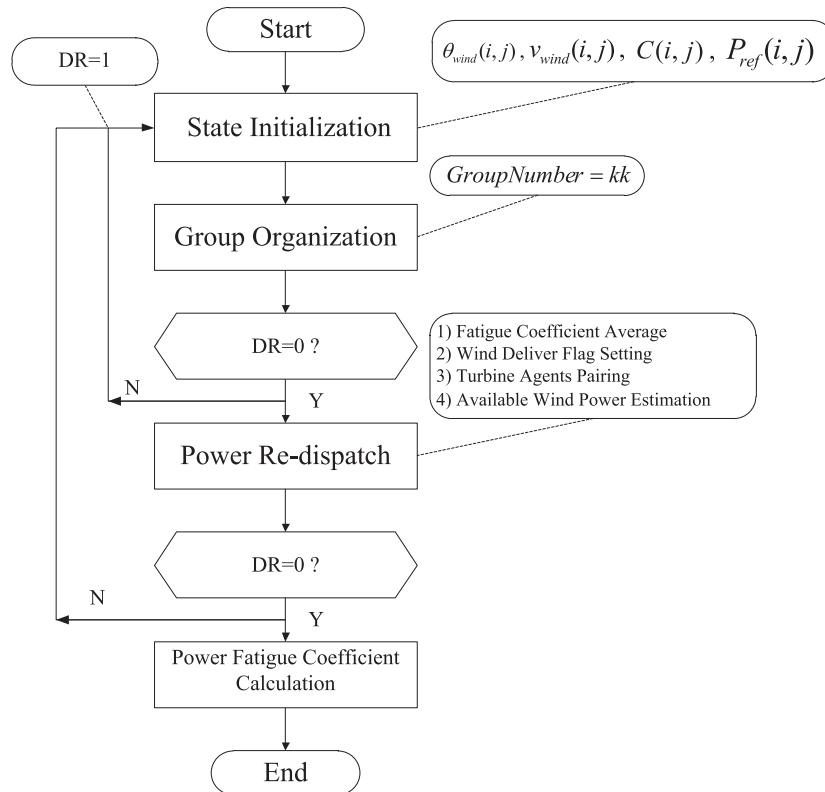


Figure 7. Work flow of an intelligent agent control.

its own fatigue coefficient from the memory of the turbine controller and the dispatched power, i.e. the reference power $P_{ref}(i; j)$. In the group organization process, the GOA arranges all the turbines along the wind direction into a group marked with kk . After the rapid group organization, the turbine controller judges the dispatch signal state from the WFMC. If the dispatch signal is $DR = 0$, no new power dispatch orders are generated. Otherwise, if the Boolean variable dispatch signal DR equals 1, all other operating states will be reset back to the initialize state.

In the former case, the intelligent agent runs ahead and enters the power re-dispatch process. This process consists of four sub-processes: fatigue coefficient average, wind deliver flag setting, turbine agents pairing and available wind power estimation. The average fatigue coefficient is sequentially calculated in an organized group. By comparing the fatigue coefficient, c , of an individual turbine agent with the group average, $\overline{c_{Group}}$, the wind delivery game variables, $\xi(i, j, k)$ and $\sigma(i, j, k)$, are determined. This expression ensures that a turbine agent with a higher fatigue coefficient can give up some of its wind power to downwind turbine agents and vice versa.

According to the fatigue coefficient, the wind delivery agent pairs are arranged so that the maximum fatigue turbine agent pairs with the minimum agent, the second highest fatigue agent pairs with the second lowest fatigue agent, and so on. In the final sub-process, the available wind power estimation calculates the power delivered to the downwind turbines and keeps the output power less than the reference power of their paired upwind turbines. The amount of delivered wind power is calculated with Equations (9) and (15).

5. ENGINEERING SIMULATIONS

In order to illustrate the intelligent agent control approach, the database of wind characteristics maintained by the Technical University of Denmark is used.³⁷ This database contains four different categories of wind data: time series of wind characteristics, time series of wind turbine responses, wind resource data and wind farm data. These time series are primarily intended for wind turbine design purposes. The data can be used for analysis of wind farm siting. In the database, we can find wind speed measurements under different conditions and for various terrain types at 55 different locations in Europe, Egypt, Japan, Mexico, Costa Rico and the USA.

We selected the Horns Rev offshore wind farm as a test case on the basis of the wind farm model shown in Figure 1. The Horns Rev site is located in the North Sea approximately 14 km off the coast. A total of 80 Vestas V80-2.0 MW units capable of producing 160 MW with an expected annual production of 600,000,000 kWh have been in operation since 2002.³⁸ The nominal wind speed is $2\text{--}24 \text{ m s}^{-1}$. The nominal turbulence intensity is between 2% and 20 %, with an average of 4.5206%. The nominal wind directions are $0\text{--}100^\circ$ and $270\text{--}360^\circ$.³⁸

By using the wind conditions described previously, the computer programmes are designed and executed in Matlab 7.1,³⁹ and a fatigue coefficient distribution is calculated on the basis of the operation data from Horns Rev. The main parameters used in our simulations are as follows:

- The average wind speed is kept at 12 m s^{-1} with a turbulence intensity of 4.5206%, from Jesper;³⁸
- γ , the ratio of the disturbance fatigue, f_{dis} , to the working fatigue, f_{work} , is 0.7;

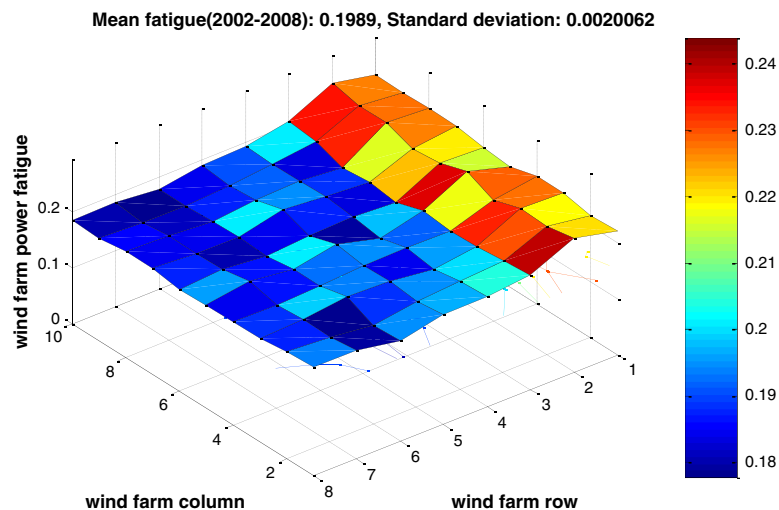


Figure 8. Conventional farm fatigue distribution (2002–2008, Horns Rev).

- Data regarding wind directions are obtained from Jesper.³⁸ The wind directions are 0° , 45° , 90° and 315° , with the tolerances estimated from Equation (28);
- Two simulation durations are used: 6 years (from 2002 to 2008) with the conventional farm control approach and 6 years (from 2008 to 2014) with the intelligent agent control approach proposed in this work;
- Any wind turbine in a group can only give its additional power to three downwind turbines in the same group because, empirically, the wind wake effect for wind turbines in a column tends to be saturated after three turbines;
- The power dispatch interval is 20 min from the farm controller;
- The reparation coefficient, p_{refp} , is equal to 0, which means that all the wind turbines are newly started from rest;
- The calculation inaccuracy for the agent group fatigue is set to 0.00001;
- The optimal target for the fatigue standard deviation in the whole offshore wind farm is less than 0.001.

In order to begin the computations, a pure zero initial distribution is used for the fatigue in December 2002 when all wind turbines had not yet yielded any electric power. By using the conventional wind farm control method,¹ the fatigue distribution, after 6 years (52560 h), is plotted in Figure 8. In Figure 8, it is seen that the distribution of the fatigue is irregular and inclined because of the natural prevailing wind conditions and the continuous far wake effect. From the expected annual production of 600,000,000 kWh (approximately 2% of Danish electricity consumption) and a wind power basic ratio between the turbines in the same column of [1, 0.6, 0.5, 0.5, 0.5, 0.5, 0.5], we can calculate the average power generated by an individual upwind turbine in the first row to be 13.0435 MWh per year.

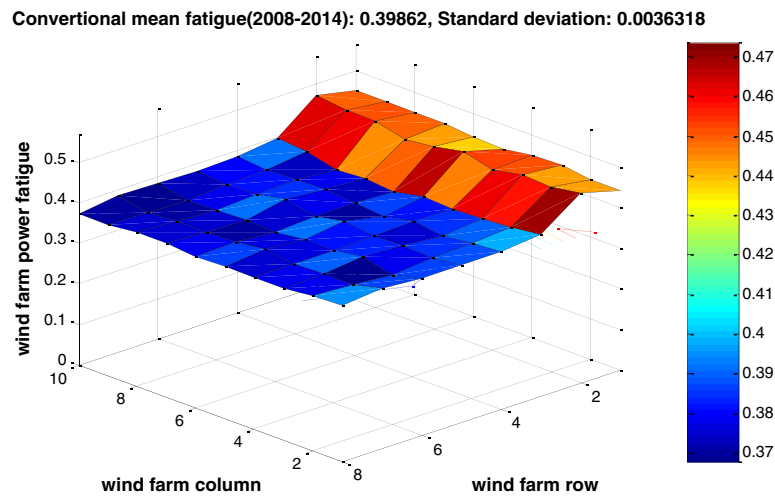


Figure 9. Farm fatigue distribution based on conventional control (2008–2014, Horns Rev).

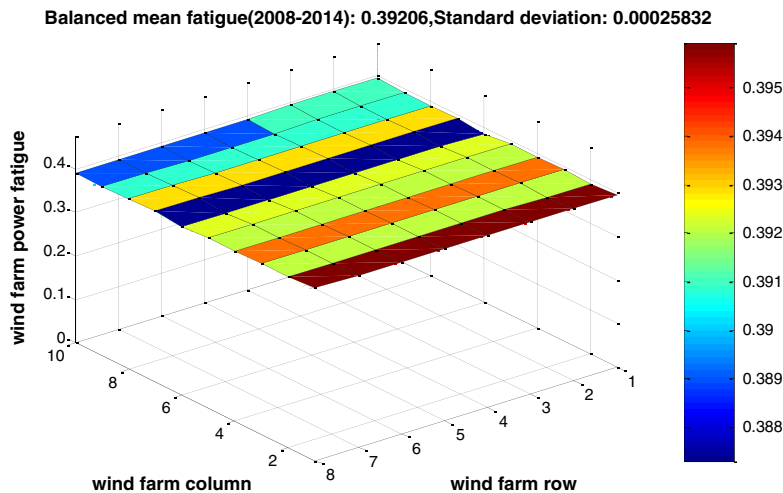


Figure 10. Farm fatigue distribution based on intelligent agent control (2008–2014, Horns Rev).

As shown in Figure 8, on the basis of the fatigue results generated for the first period, 2002–2008, the mean fatigue of the entire wind farm is 0.1989, and the standard deviation of the farm fatigue distribution is 0.0020062.

The fatigue distribution development for the second period, 2008–2014, is shown in Figures 9 and 10. The simulation with the conventional control method is shown in Figure 9. The mean fatigue of the entire wind farm increases to 0.39862, and the standard deviation of the farm fatigue distribution increases to 0.0036318.

In order to balance the wind turbine fatigue, power re-dispatch is implemented using intelligent agent control. The optimized result, shown in Figure 10, indicates that the mean fatigue of the entire wind farm increases to 0.39206, and the standard deviation of the farm fatigue distribution decreases to 0.00025832.

These results indicate that, although more fatigue occurs than in the earlier period (2002–2008) because of the increased electric power generation and the basic wind disturbance, the turbine fatigue distribution is flatter. Here, the fatigue distribution mesh colour appears irregular, but the scale colour bar only varies from 0.388 to 0.395, which is a far smaller variation than that shown in Figure 9. Furthermore, the small colour variation shows that the natural effects of random wind disturbances still exist.

6. DISCUSSIONS

The fatigue optimization is a constrained problem. One constraint is that the average fatigue for every turbine (we call it the mean fatigue in Figures 8, 9 and 10) should be smaller than the fatigue generated by conventional control. Another is that the total power loss should be restricted to be a few per cent of the total dispatched power in every power dispatch interval.

In theory, because of the wind power delivery coefficients, a small part of wind energy is lost in the wind power delivery between the upwind and downwind turbines. These power delivery coefficients are the normal delivery coefficient (0.8012) and oblique delivery coefficient (0.8346). As a consequence, the maximum turbine fatigue is smaller with the proposed approach.

The fatigue distribution development for the second period, 2008–2014, was shown in Figures 9 and 10. In the first case, the numerical simulation with the conventional control method showed that the mean fatigue of the entire wind farm increases to 0.39862. In the second case, the optimized result indicated that the mean fatigue of the entire wind farm is 0.39206. The numerical examples, hence, show that the average fatigue is smaller in the intelligent agent balanced approach than in the conventional approach.

This paper proposes an optimization of fatigue distribution with an empirical value of 0.7 for the parameter γ , which is the ratio of the disturbance fatigue, f_{dis} , to the working fatigue, f_{work} , for the 8×10 turbine in the Horns Rev example. The ratio of wind disturbance fatigue to power fatigue should vary according to the wind farm layout and the local wind conditions. The ratio of disturbance fatigue to working fatigue, shown in Figures 11 and 12, is supported by data from the comparison of the conventional and balanced fatigue distributions (Table A.1) in the appendix.

In Figure 11, the dotted curve is the conventional fatigue, and the solid curve is the balanced fatigue. When using the same wind farm data for the second period (2008–2014), the two curves vary with the ratio of the turbulence fatigue to the

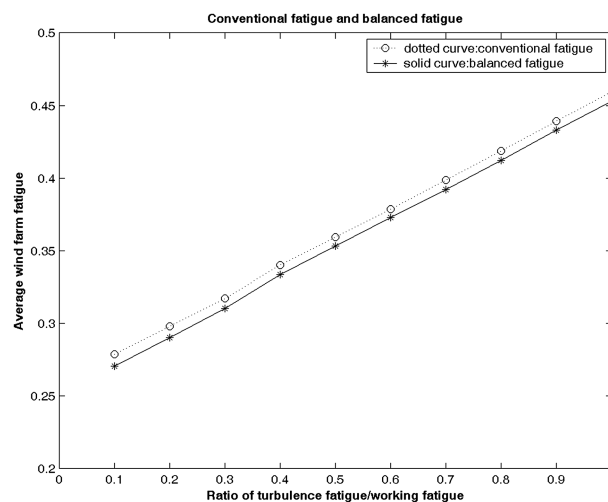


Figure 11. Average wind farm fatigue obtained using the conventional and intelligent agent control approaches (2008–2014, Horns Rev).

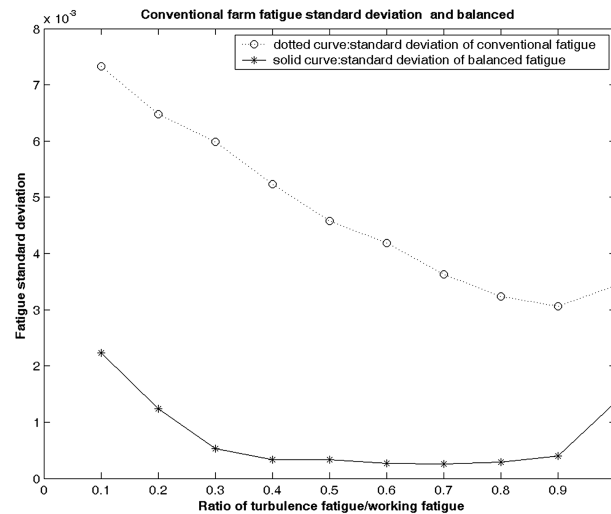


Figure 12. Standard deviation of the wind farm fatigue (2008–2014, Horns Rev).

working fatigue, γ . The ratio γ varies from 0.1 to 10 for the 19 points shown in Table A.1, and the average farm fatigue for a selection of γ between 0.1 and 1 is shown in Figure 11. It is seen that in the optimized case, the balanced fatigue is always slightly lower than the corresponding conventional fatigue, regardless of the value of γ . It is worth noting the fact that the intelligent agent optimization does not significantly reduce the wind farm fatigue, which also means that the wind power loss is relatively low.

In Figure 12, the dotted curve is the standard deviation curve of the conventional method fatigue, and the solid curve is the standard deviation curve of the balanced method fatigue. Both curves vary with the ratio of the turbulence fatigue to the working fatigue, γ , which ranges from 0.1 to 1.0. It is seen that in the optimized result, the standard deviation curve for the balanced fatigue method is always lower than that for the corresponding conventional fatigue method and is much lower than that in the case shown in Figure 11, regardless of the value of γ . The standard deviation reaches a minimum of 0.00025832 when γ is 0.7 for the standard deviation curve of the balanced fatigue method.

Both Figures 11 and 12 show that the fatigue optimization model used in the multi-agent control in this paper is feasible and effective and can be used in other wind farms.

For the first period, the power generation of the entire wind farm was computed for a wind turbulence of 4.5206%, as described in Jesper.³⁸ In the same wind conditions, the power loss in the fatigue balance period (2008–2014) is less than 9.15% of the original reference power (the sum of the power dispatched to the individual wind turbines) for $\gamma = 0.1$ and is typically 4.49% for $\gamma = 0.7$, which occurs during the wind delivery process. Compared with the cost associated with frequent and expensive maintenance, empirically, a power loss is acceptable to some extent.

The standard deviation of the fatigue will be lower and the fatigue distribution will be flatter when using the intelligent agent control approach. The fatigue process for the wind turbines will be synchronized, resulting in lower maintenance costs and an increased lifespan for the offshore wind farm. If we consider other wind directions beyond the permitted angle tolerances, the overlapping wake effect will be too complex. In this case, we may use the same intelligent agent approach proposed in this work to operate in a simplified organization mode in which any power delivery group consists of two wind turbines, one acting as the GOA and the other as the GMA. The rest of the calculation is similar, as previously mentioned.

At Horns Rev, the WFMC manages the requirements of power control. The WFMC communicates with the turbines and the remote control system via an ethernet TCP/IP-based network. All communication to and from the WFMC is handled through an OPC interface via this network.³⁹ In the conventional control approach, an essential parameter in the control structure is the power capability of both the individual turbines and the wind farm as a whole. Each turbine determines its own active and reactive power capability from an estimated 'free wind speed' in front of the turbine. This wind speed estimation is based on the knowledge of the actual pitch angle, power and rotor speed.

In the approach proposed in this paper, the wind turbines can act as intelligent agents that communicate with each other via an OPC interface standard, self-organize into wind power delivery groups and re-dispatch the power in each group for fatigue optimization. Finally, each turbine determines its own active and reactive power capability from an estimated 'wake wind speed' in front of the turbine. The algorithm added to the self-communication and the power re-dispatch can be implemented in each wind turbine controller; therefore, no additional computational burden will be applied to the WFMC, which guarantees conventional control and communication efficiency in the entire wind farm network.

7. CONCLUSIONS

In this paper, a novel approach based on an intelligent agent control has been developed for fatigue optimization in an offshore wind farm. Some conclusions can be drawn, as follows.

First, the operation and maintenance costs for offshore wind farms are significant contributors to the cost of energy. Unbalanced fatigue is one of the causes leading to these high maintenance costs. Balancing the fatigue process is a new approach and could be used to reduce maintenance frequency and, thereby, the cost of energy.

Second, with individual wind turbine controllers, the intelligent agent control approach allows the use of GOAs to adaptively organize GMAs into different wind delivery groups according to the wind direction without conflicting with the WPMC. The re-dispatched power can be calculated by the GOAs in the individual groups and can be sent to the WPMC.

Third, the intelligent agent control programme of this new approach can be executed and distributed in the wind turbine controllers on the basis of the current wind farm network. This approach can operate without additional computational burdens on the farm controller. This paradigm agrees with the idea of decentralized control.

Fourth, the numerical example shows that the intelligent agent control approach is capable of optimizing the fatigue distribution of an offshore wind farm. Considering the seasonal and cyclic climate condition, by increasing the intelligent agent control period, the fatigue distribution could be flatter, which results in lower maintenance frequency for the offshore wind farm.

ACKNOWLEDGEMENTS

This work was supported by the Danish Ministry of Science, Technology and Innovation CIRIUS (Grant No. 2007-7232-12), the Scientific Research Foundation for Returned Overseas Chinese Scholars, State Education Ministry (2010), the Science and Technology Commission of Shanghai Key Basic Research Project (Grant No. 10JC1415200), the 2010 Shanghai manufacturing information for special projects (Grant No. 10DZ1122402), the Shanghai Leading Academic Discipline Project (Grant No. B004) and the National Natural Science Foundation Project of China (Grant No. 50905129). The authors wish to thank the researchers at the section of Automation and Control of Aalborg University. In addition, the Technical University of Denmark is acknowledged for providing the wind data.

APPENDIX A.

Table A.1. Comparison of the conventional and balanced fatigue distributions (2008–2014).

γ	0.1	0.2	0.3	0.4	0.5	0.6	
c_a_fat	0.27891	0.29804	0.31736	0.34005	0.35921	0.37883	
b_a_fat	0.27075	0.29037	0.31048	0.33345	0.35327	0.37293	
c_std	0.007326	0.006481	0.005989	0.005235	0.004574	0.004184	
b_std	0.002236	0.001237	0.000524	0.000337	0.000328	0.000267	
γ	0.7	0.8	0.9	1	2	3	
c_a_fat	0.39862	0.41896	0.43908	0.45951	0.66333	0.8662	
b_a_fat	0.39207	0.41241	0.43299	0.45324	0.66163	0.86278	
c_std	0.003632	0.003231	0.003057	0.003433	0.010223	0.018621	
b_std	0.000258	0.000287	0.000393	0.001357	0.010281	0.018528	
γ	4	5	6	7	8	9	10
c_a_fat	1.0656	1.2695	1.4732	1.6722	1.8738	2.0804	2.2841
b_a_fat	1.0624	1.2668	1.4717	1.6697	1.866	2.0777	2.2764
c_std	0.027335	0.036352	0.045218	0.053479	0.062257	0.070714	0.07997
b_std	0.027233	0.036245	0.04524	0.053345	0.06183	0.070564	0.079596

Note: γ is the ratio of the disturbance fatigue, f_{dis} , to the working fatigue, f_{work} ; c_a_fat is the conventional average fatigue; b_a_fat is the balanced average fatigue; c_std is the standard deviation of farm fatigue distribution based on conventional power control; b_std is the standard deviation of farm fatigue distribution based on balanced power control.

REFERENCES

1. Kristoffersen JR, Christiansen P. Horns Rev offshore windfarm: its main controller and remote system. *Wind Engineering* 2003; **27**: 351–360.
2. German Energy Agency (dena). *Integration into the National Grid of Onshore and Offshore Wind Energy Generated in Germany by the Year 2020*. Dena Press: Berlin, 2002.
3. Slootweg JG, Kling WL. Is the answer blowing in the wind? *IEEE Power and Energy Magazine* 2003; **1**: 26–33.
4. Hau E. *Wind Turbines-fundamentals, Technologies, Application, Economics*. Springer-Verlag Berlin Heidelberg: Berlin, 2006.
5. Tong KC. Technical and economic aspects of a floating offshore wind farm. *Journal of Wind Engineering and Industrial Aerodynamics* 1998; **74**: 399–410.
6. Quinonez-Varela G, Ault GW, Anaya-Lara O, McDonald JR. Electrical collector system options for large offshore wind farms. *Renewable Power Generation, IET* 2007; **1**: 107–114.
7. Cockerill TT, Kuhn M, van B G J W, Bierboomsc W, Harrison R. Combined technical and economic evaluation of the northern European offshore wind resource. *Journal of Wind Engineering and Industrial Aerodynamics* 2001; **89**: 689–711.
8. Fernandez RD, Mantz RJ, Battaiotto PE. Contribution of wind farms to the network stability, *Proceedings of IEEE Power Engineering Society General Meeting*, Montreal, 2006; 2–8.
9. Nilsson J, Bertling L. Maintenance management of wind power systems using condition monitoring systems-life cycle cost analysis for two case studies. *IEEE Transactions on Energy Conversion* 2007; **22**: 223–229.
10. Shirani M, Häkegård G. Fatigue life distribution and size effect in ductile cast iron for wind turbine components. *Engineering Failure Analysis* 2011; **18**: 12–24.
11. Marín JC, Barroso A, París F, Cañas J. Study of fatigue damage in wind turbine blades. *Engineering Failure Analysis* 2009; **16**(2): 656–668.
12. Sørensen JD, Frandsen S, Tarp-Johansen NJ. Effective turbulence models and fatigue reliability in wind farms. *Probabilistic Engineering Mechanics* 2008; **23**(4): 531–538.
13. Barle J, Grubisic V, Radica D. Service strength validation of wind-sensitive structures, including fatigue life evaluation. *Engineering Structures* 2010; **32**(9): 2767–2775.
14. van der H E L, Schaak P, van E T V. Wind turbine control algorithms. *ECN Technical report, RX-03-37*, Dutch Ministry of Economic Affairs:Petten, Holland, 2003.
15. Leithead W, Dominguez S, Spruce C. Analysis of tower/blade interaction in the cancellation of the tower fore-aft mode via control, *Proceedings of European Wind Energy Conference*, London, 2004; 1–10.
16. Leithead WE, Connor B. Control of variable speed wind turbines: design task. *International Journal of Control* 2000; **13**: 1189–1212.
17. Camblong H. *Minimization of the Impact of Wind Disturbances in Variable Speed Wind Turbine Power Generation*, PhD Dissertation (in French), ENSAM and University of Mondragon, 2003.
18. Lescher F, Camblong H. LPV control of wind turbines for fatigue loads reduction using intelligent micro sensors, *Proceedings of American Control Conference*, New York City, 2007; 6061–6066.
19. Trudnowski D, Lemieux D. Independent pitch control using rotor position feedback for wind-shear and gravity fatigue reduction in a wind turbine, *Proceedings of the American Control Conference*, Anchorage, 2002; 4335–4340.
20. Kallesøe BS. A low-order model for analysing effects of blade fatigue load control. *Wind Energy* 2006; **9**: 421–436.
21. Heege K, Betran J, Radovic Y. Fatigue load computation of wind turbine gearboxes by coupled finite element, multi-body system and aerodynamic analysis. *Wind Energy* 2007; **10**: 395–413.
22. Veldkamp HF, van der T J. Influence of wave modelling on the prediction of fatigue for offshore wind turbines. *Wind Energy* 2005; **8**: 49–65.
23. Thomsen K, Soerensen P. Fatigue loads for wind turbines operating in wakes. *Journal of Wind Engineering and Industrial Aerodynamics* 1999; **80**: 121–136.
24. Russell SJ, Norvig P. *Artificial Intelligence: A Modern Approach*, 2nd ed. Prentice Hall: Upper Saddle River, New Jersey, (2003).
25. Krishna V, Ramesh VC. Intelligent agents for negotiations in market games, Part 2: model. *IEEE Transactions on Power Systems* 1998; **13**: 1109–1114.
26. Bryant BD, Miikkulainen R. Evolving stochastic controller networks for intelligent game agents, *Proceedings of IEEE Congress on Evolutionary Computation*, Sheraton Vancouver, 2006; 1007–1014.

27. Frandsen ST. Turbulence and turbulence generated structural loading in wind turbine clusters, *Risø National Laboratory*, Roskilde, Denmark, January 2007; 22–56.
28. Templin RJ. An estimation of the interaction of windmills in widespread arrays. *Laboratory Report LTR-LA-171, National Aeronautical Establishment*, 1974.
29. Newman BG. The spacing of wind turbines in large arrays. *Journal of Energy Conversion* 1977; **16**: 169–171.
30. Bossanyi EA, Maclean C, Whittle GE, Dunn PD, Lipman NH, Musgrove PJ. The efficiency of wind turbine clusters, *Proceedings of Third International Symposium on Wind Energy Systems (BHRA)*, Copenhagen, 1980; 401–416.
31. Frandsen S. On the wind speed reduction in the center of large clusters of wind turbines. *Journal of Wind Engineering and Industrial Aerodynamics* 1992; **39**: 251–265.
32. Emeis S, Frandsen S. Reduction of horizontal wind speed in a boundary layer with obstacles. *Boundary Layer Meteorol* 1993; **64**: 297–305.
33. Vermeera LJ, Sørensen JN, Crespo A. Wind turbine wake aerodynamics. *Progress in Aerospace Sciences* 2003; **39**: 467–510.
34. MILBORROW DJ. The performance of arrays of wind turbines. *Journal of Industrial Aerodynamics* 1980; **5**: 403–430.
35. Saida NM, Mhiria H, Bournotb H, Palecb GL. Experimental and numerical modelling of the three-dimensional incompressible flow behaviour in the near wake of circular cylinders. *Journal of Wind Engineering and Industrial Aerodynamics* 2008; **96**: 471–502.
36. UML, <http://www.omg.org/technology/documents/formal/uml.htm>.
37. Winddata-Offshoremeasurements, 2008. <http://www.winddata.com/>.
38. Jesper RK. The Horns Rev wind farm and the operational experience with the wind farm main controller. *Copenhagen Offshore Wind* October 2005; **2005**: 26–28.
39. Matlab7.1Release, 2008. <http://www.mathworks.com>.